A Stochastic Geometric Analysis of Device-to-Device Communications Operating Over Generalized Fading Channels

Young Jin Chun, *Member, IEEE*, Simon L. Cotton, *Senior Member, IEEE*, Harpreet S. Dhillon, *Member, IEEE,* Ali Ghrayeb, *Senior Member, IEEE*, and Mazen O. Hasna, *Senior Member, IEEE*

***Abstract*— Device-to-device (D2D) communications are now considered an integral part of future 5G networks, which will enable direct communication between user equipments and achieve higher throughputs than conventional cellular networks, but with the increased potential for co-channel interference. The physical channels, which constitute D2D communications, can be expected to be complex in nature, experiencing both line-of-sight (LOS) and non-LOS conditions across closely located D2D pairs. In addition to this, given the diverse range of operating environments, they may also be subject to clustering of the scattered multipath contribution, *i.e.*, propagation characteristics which are quite dissimilar to conventional Rayleigh fading environments. To address these challenges, we consider two recently proposed generalized fading models, namely κ-μ and η-μ, to characterize the fading behavior in D2D communications. Together, these models encompass many of the most widely utilized fading models in the literature such as Rayleigh, Rice (Nakagami-n), Nakagami-m, Hoyt (Nakagami-q), and One-sided Gaussian. Using stochastic geometry, we evaluate the spectral efficiency and outage probability of D2D networks under generalized fading conditions and present new insights into the tradeoffs between the reliability, rate, and mode selection. Through numerical evaluations, we also investigate the performance gains of D2D networks and demonstrate their superiority over traditional cellular networks.**

***Index Terms*— 5G, device-to-device network, η-μ fading, κ-μ fading, rate-reliability trade-off, stochastic geometry.**

Manuscript received May 13, 2016; revised October 29, 2016 and February 26, 2017; accepted March 13, 2017. Date of publication March 30, 2017; date of current version July 10, 2017. The work of Y. J. Chun and S. L. Cotton was supported in part by the Engineering and Physical Sciences Research Council under Grant EP/L026074/1 and the Department for the Economy Northern Ireland under Grant USI080. The work of H. S. Dhillon was supported by the U.S. National Science Foundation under Grants CCF-1464293 and CNS-1617896. The work of M. O. Hasna was supported by the NPRP Grant 4-1119-2-427 from the Qatar National Research Fund (a member of Qatar Foundation). The statements made herein are solely the responsibility of the authors. The associate editor coordinating the review of this paper and approving it for publication was J. M. Romero Jerez. *(Corresponding author: Young Jin Chun.)*

Y. J. Chun and S. L. Cotton are with the Wireless Communications Laboratory, ECIT Institute, Queen's University Belfast, Belfast, BT3 9DT, U.K. (e-mail: y.chun@qub.ac.uk; simon.cotton@qub.ac.uk).

H. S. Dhillon is with Wireless@VT, Department of Electrical and Computer Engineering, Virginia Tech, Blacksburg, VA 24061 USA (e-mail: hdhillon@vt.edu).

A. Ghrayeb is with the Department of Electrical and Computer Engineering, Texas A&M University at Qatar, Doha, Qatar (e-mail: ali.ghrayeb@qatar.tamu.edu).

M. O. Hasna is with the Department of Electrical Engineering, Qatar University, Doha, Qatar (e-mail: hasna@qu.edu.qa).

Color versions of one or more of the figures in this paper are available online at http://ieeexplore.ieee.org.

Digital Object Identifier 10.1109/TWC.2017.2689759

I. Introduction

A. Related Works

THE recent unprecedented growth in mobile traffic has compelled the telecommunications industry to come up with new and innovative ways to improve cellular network performance to meet the ever increasing data demands. This has led to the introduction of fifth generation (5G) networks which are expected to provide 1000 fold gains in capacity while achieving latencies of less than 1 millisecond [1]. Device-to-device communications are a strong contender for 5G networks [2] that allow direct communication between user equipments (UEs) without unnecessary routing of traffic through the network infrastructure, resulting in shorter transmission distances and improved data rates than traditional cellular networks [3].

Currently, D2D communication is standardized by the 3rd Generation Partnership Project (3GPP) in LTE Release 12 to provide proximity based services and public safety applications [4]. In parallel to the standardization efforts, D2D communications have been actively studied by the research community. For example, in [5], the authors have proposed D2D as a multi-hop scheme, while in [6] and [7], the work conducted in [5] has been extended to demonstrate that D2D communications can improve spectral efficiency and the coverage of conventional cellular networks. Additionally, D2D has also been applied to multi-cast scenarios [8], machine-to-machine (M2M) communications [9], and cellular off-loading [10].

While D2D communications offer many advantages, they also come with numerous challenges. These include the difficulties in accurately modeling the interference induced by cellular and D2D UEs, and consequently optimizing the resource allocation based on the interference model. Most of the previous works published in this area have relied on system-level simulations with a large parameter set [11], meaning that it is difficult to draw general conclusions. Recently, stochastic geometry has received considerable attention as a useful mathematical tool for interference modeling. Specifically, stochastic geometry treats the locations of the interferers as points distributed according to a spatial point process [12]. Such an approach captures the topological randomness in the network geometry, offers high analytical flexibility and achieves accurate performance evaluation [13]–[17].

Much work has also been done on evaluating the performance of D2D networks over Rayleigh fading channels. In [18], the authors have compared two D2D spectrum sharing schemes (overlay and underlay) and evaluated the average achievable rate for each scheme based on the stochastic geometric framework. In [19], the authors extended the work conducted in [18] by considering a D2D link whose length depends on the user density. In [20], the authors proposed a flexible mode selection scheme which makes use of truncated channel inversion based power control for underlaid D2D networks. Notwithstanding these advances, limited work has been conducted to consider D2D networks with general fading channels, for example in [21], the authors have considered underlaid D2D networks over Rician fading channels and evaluated the success probability and average achievable rate.

B. Motivation and Contributions

In 5G networks and especially for D2D communications, fading environments will range from homogeneous and circularly symmetric through to non-homogeneous and non-circularly symmetric. For example, the METIS project has already demonstrated that the physical channels of 5G networks can be inhomogeneous with clusters of non-circularly symmetric scattered waves [22]. Clearly in this case, the assumption of traditional, homogeneous, linear and single cluster fading models such as Rayleigh will no longer be sufficient and we must look towards other more general and realistic models such as κ-μ [23]–[25] and η-μ [23], [26]. Influenced by this, we consider the κ-μ fading model which accounts for homogeneous, linear environments with line-of-sight (LOS) components and multiple clusters of scattered signal contributions, while the η-μ fading model represents inhomogeneous, linear environments with non-line-of-sight (NLOS) conditions and multiple clusters of scattered signal contributions.

As discussed earlier, most of the existing work in stochastic geometry for wireless networks has been focused on Rayleigh fading environments, owing to its tractability and favorable analytical characteristics. The signal-to-noise-plus-interference ratio (SINR) distributions for general fading environments require evaluating the sum-products of aggregate interference where several approaches have been proposed to facilitate the derivation, most notably:

1) The *conversion method* based on displacement theorem was used in [27]–[30]. This method treats the channel randomness as a perturbation in the location of the transmitter and transforms the original network with arbitrary fading into an equivalent network without fading. Although the conversion method can be applied to any fading distribution, it is more tractable for handling large-scale shadowing effects. Specifically, if one applies the conversion method to small-scale fading, the resulting equivalent model will have no fading, thereby the Laplace transform-based approach can not be utilized.
2) The *series representation method* was used in [21] and [31]. This approach expresses the interference functionals as an infinite series of higher order derivative terms [32] given by the Laplace transform of the interference power. While the series representation method provides a tractable alternative for handling general fading, it often leads to situations where it is difficult to derive closed form expressions.
3) The *integral transform based approach* was used in [33]–[35], where either the Fourier transform (FT), Laplace transform (LT), characteristic function (CF) or moment generating function (MGF) is utilized. For instance, Gil-Pelaez's inversion formula was used in [33] to find the distribution of the SINR using the MGF. However, Gil-Pelaez's inversion formula involves an integral over the complex plane and the MGFs of the related random variables may not always exist. The Plancherel-Parseval theorem was used in [34] and [35] to calculate the expectation of an arbitrary function of the interference using the FT (or LT). Although the Plancherel-Parseval theorem provides a general framework, it often involves complex multi-fold integration and results in intractable expressions.

Motivated by these approaches and their limitations, we adopt a stochastic geometric framework to facilitate the performance evaluation of D2D networks over generalized fading channels; namely, κ-μ and η-μ. We consider a D2D network overlaid upon a cellular network where the spatial locations of the mobile UEs as well as the base stations (BSs) are modeled as Poisson point processes (PPPs). The adopted framework can evaluate the average of an arbitrary function of the SINR, thereby enabling the estimation of the average rate and outage probability.

The main contributions of this paper may be summarized as follows.

1) We consider generalized fading conditions, namely, (i) κ-μ and (ii) η-μ fading, to account for various small-scale fading effects, such as LOS/NLOS conditions, multipath clustering, and power imbalance between the in-phase and quadrature signal components. These two models together encompass most of the popular fading models proposed in the literature. We utilize the series representation of the κ-μ and η-μ distributions to improve tractability and achieve closed form expressions.
2) We analyze the Laplace transform of the interference over κ-μ and η-μ fading channels and derive a closed form expression for the D2D and cellular links. By using a channel inversion based power control, we derive the Laplace transform of the interference in a closed form that does not involve an integral expression.
3) We exploit a novel stochastic geometric approach for evaluating the performance of D2D networks over generalized fading channels. This approach enables us to evaluate the average of an arbitrary function of the SINR as a closed form expression. We invoke the proposed stochastic geometric approach to evaluate the spectral efficiency and outage probability of D2D networks and compare that to the performance of conventional cellular networks. Furthermore, we study the trade-off among a number of performance metrics,

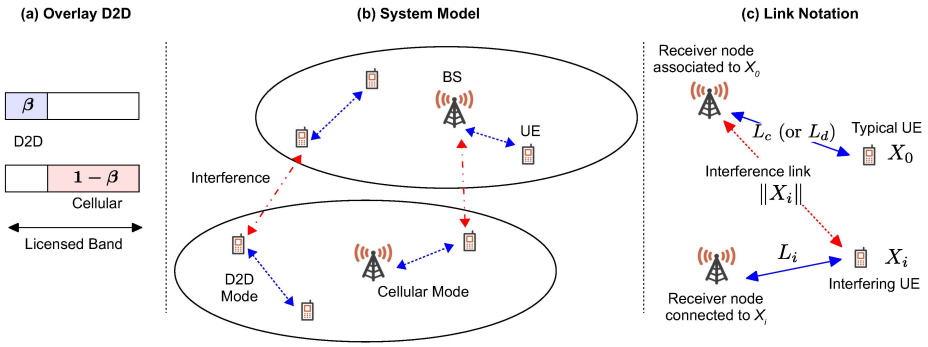

Fig. 1. System Model for Overlaid D2D Network.

which can provide invaluable insights that may be used to optimize future network design.

The remainder of this paper is organized as follows. We describe the system model in Section II and the generalized fading models in Section III. We introduce the interference of cellular and D2D networks in Section IV, then utilize a stochastic geometric approach to evaluate the spectral efficiency and the outage probability of D2D networks in Section V. We present numerical results in Section VI and conclude the paper in Section VII with some closing remarks.

II. System Model

A. Network Model

We consider a D2D network overlaid upon an uplink cellular network where a UE can directly communicate with other UEs without relying on the cellular infrastructure if a certain criterion is met. The overlaid spectrum access scheme allocates orthogonal time/frequency resources to the cellular and D2D transmitters by dividing the uplink spectrum into two non-overlapping portions. The overlay D2D network excludes cross-mode interference between cellular and D2D UEs and achieves a reliable link quality at the cost of lower spectrum utilization. Specifically, a fraction β of the spectrum is assigned for D2D communications and the remaining $1-\beta$ is allocated to cellular communications, where $0 \leq \beta \leq 1$.

Fig. 1 depicts a high level overview of the system model where the locations of the nodes are modeled as a spatial point process in $\mathbb{R}^2$. The UEs are assumed to form a homogeneous PPP $\Phi \equiv \{X_i\}$[1] with intensity λ and each UE X_i has associated parameters that collectively form a marked PPP $\tilde{\Phi}$ as follows

$$\tilde{\Phi} = \{(X_i, \varrho_i, L_i, P_i)\}, \tag{1}$$

where L_i is the distance between the i-th UE and its intended receiver (referred to henceforth as the *link distance*), and P_i is the transmit power of the i-th UE. The parameter ϱ_i indicates the inherent type of the i-th transmit UE which may be a potential D2D UE with probability $q = P(\varrho_i = 1)$, or a cellular UE with probability $1-q$, where $q \in [0,1]$. For notational simplicity, we denote by L_c the link length between a typical cellular UE and the associated BS. Similarly, L_d represents the link length between a typical D2D UE and the D2D receiver UE. The receiver can be either a cellular BS or D2D receiver UE depending on the associated UE type. The cellular BSs are assumed to be uniformly distributed as PPP Ψ with intensity λ_b. The D2D receiver UEs are randomly distributed around their associated D2D UE according to the distribution of the link length L_d, which is described later in (6). The performance analysis is performed for the typical receiver, which is assumed to be located at the origin due to the stationarity of this setup. The notations used in this paper are summarized in Table I.

[1] X_i will be used to denote both the i-th UE and the coordinate of its position.

B. Mode Selection and UE Classification

The operating mode of the UE $X_i \in \tilde{\Phi}$ is determined by two factors; 1) the inherent type (ϱ_i) and 2) the mode selection policy. If $\varrho_i = 0$, then the UE X_i is a cellular UE and always connects to its closest BS (which is equivalent to the so-called maximum average received power association). If $\varrho_i = 1$, then X_i is a potential D2D UE which may use either cellular or D2D mode based on the adopted mode selection policy.

We assume a distance-based mode selection scheme [18]. That is, a potential D2D UE chooses the D2D mode if the D2D link length is smaller than or equal to a predefined mode selection threshold θ, *i.e.*, $L_d \leq \theta$. Otherwise, cellular mode is selected. Therefore, the complete set of transmit UEs $\tilde{\Phi}$ can be divided into two spatial point processes as follows

- UEs operating in cellular mode:

$$\Phi_c \text{ with intensity } \lambda_c = [(1-q) + q\mathrm{P}(L_d > \theta)]\,\lambda, \tag{2}$$

- UEs operating in D2D mode:

$$\Phi_d \text{ with intensity } \lambda_d = q\mathrm{P}(L_d \leq \theta)\lambda. \tag{3}$$

1) Cellular Mode: We assume full-buffer transmission and orthogonal multiple access in the cellular uplink implying that *at most* one transmitter is active per cell over a given resource block. The locations of the active UEs (in the cellular mode) scheduled over the same resource block as the typical receiver are assumed to follow the point process $\Phi_c^e \subset \Phi_c$. Due to the restriction that at most one point of Φ_c^e can lie in each cell of the Poisson Voronoi tessellation formed by Ψ, it is not straightforward to characterize Φ_c^e. This is one of the key reasons why the *exact* uplink analysis for this setup has not yet been performed. Interested readers are advised to refer to [36] for more detailed discussion on user

TABLE I
COMMON SYSTEM PARAMETERS

Parameter	Description	Value
β	Spectrum partition factor	0.2
θ	Mode selection threshold	100 m
ε	ALOHA transmit probability	0.8
α	Path-loss exponent ($\delta = \frac{2}{\alpha}$)	4
τ	Reference path-loss at the unit distance	
N_0	Noise power spectral density ($N = \frac{N_0}{\tau}$)	$N = -60$ (dBm/Hz)
ϱ_i	Inherent type of the i-th UE - Potential D2D UE with probability $q = P(\varrho_i = 1)$, or cellular UE with probability $1 - q$	$q = 0.2$
ξ	D2D link distance fitting parameter	
T_o	Predefined SINR threshold	
M	Number of potential cellular UEs within a cell	
G	Small-scale fading coefficient, *i.e.*, squared signal envelope ($\bar{w} = \mathbb{E}[G]$)	$\bar{w} = 1$
κ	Ratio between the total power of the dominant components and the scattered waves	
μ	Real-valued extension of the number of multi-path clusters	
η	The scattered-wave power ratio between the in-phase and quadrature components - $h = \frac{2+\eta+\eta^{-1}}{4}$, $H = \frac{\eta^{-1}-\eta}{4}$ [23] - $\Omega_{\kappa\mu} = \frac{\bar{w}}{\mu(1+\kappa)}$, $\Omega_{\eta\mu} = \frac{\bar{w}}{2\mu h}$	
Φ	Set of the transmit UEs with intensity λ	$\lambda = \frac{10}{\pi 500^2}$
Ψ	Set of the cellular BSs with intensity λ_b	$\lambda_b = \frac{1}{\pi 500^2}$
Φ_c	Set of UEs operating in the cellular mode with intensity λ_c	
Φ_d	Set of UEs operating in the D2D mode with intensity λ_d	
$\hat{\Phi}_c$	Approximation to the set of active interfering UEs in the cellular mode that are scheduled in the same orthogonal resource block as the typical UE	
L_i	Link length of the i-th UE	
L_c	Link length between a typical cellular UE and the associated BS	
L_d	Link length between a typical D2D UE and the D2D receiver UE	
P_i	Transmit power of the i-th UE	
P_c	Transmit power of the UEs operating in the cellular mode	
P_d	Transmit power of the potential D2D UEs in the D2D mode	
$\bar{P}_d$	Transmit power of an arbitrary potential D2D UE - $\bar{P}_d = \mathrm{P}(L_d \le \theta) P_d + \mathrm{P}(L_d > \theta) P_c$	
R_c	Spectral efficiency of a cellular UE	
R_d	Spectral efficiency of a potential D2D UE operating in D2D mode	
$\bar{R}_d$	Spectral efficiency of a potential D2D UE - $\bar{R}_d = \mathrm{P}(L_d > \theta) R_c + \mathrm{P}(L_d \le \theta) R_d$	

distributions in cellular networks. For high user densities, one generative model that closely emulates this scenario while also being quite realistic from the actual system perspective is to assume that there is *exactly* one point of Φ_c^e in each cell of the Poisson Voronoi tessellation formed by Ψ (also assumed to be uniformly distributed in that cell). Viewed this way, Φ_c^e can be thought of as a *Poisson-Voronoi perturbed lattice* [37]. However, due to the correlation between Φ_c^e and Ψ (which correlates various link distances), the exact analysis for even this setup is also not known. That being said, it is possible to capture some of this correlation by approximating Φ_c^e with a non-homogeneous PPP $\hat{\Phi}_c$ with a distance-dependent intensity function. This uplink model was introduced and exploited in [13] and [38]–[40] and has been shown to provide a reasonable approximation for the SINR distribution of the cellular link. Please refer to [13] and [38] for more details about the uplink problem and this approximation approach.

Assumption 1: *Given that the typical receiver is located at the origin, the set of active interfering UEs Φ_c^e in the cellular mode that are scheduled within the same resource block is approximated by a non-homogeneous PPP $\hat{\Phi}_c$ with intensity $\hat{\lambda}_c = \lambda_b \left(1 - \exp\left(-\pi \lambda_b d^2\right)\right)$ where $\|X_i\| = d$ is the distance between the interfering UE and the origin, as illustrated in Fig. 1(c). The link distances L_c and L_i can be approximately modeled by the Rayleigh distribution [13] as follows*

$$\begin{aligned} f_{L_c}(r) &= 2\pi\lambda_b r \exp\left(-\lambda_b \pi r^2\right), \\ \mathrm{P}\left(L_c \le r\right) &= 1 - \exp\left(-\lambda_b \pi r^2\right), \end{aligned} \tag{4}$$

$$f_{L_i}\left(r \,|d\right) = \frac{2\pi\lambda_b r \exp\left(-\lambda_b \pi r^2\right)}{1 - \exp\left(-\lambda_b \pi d^2\right)}, \quad 0 \le r \le d, \tag{5}$$

where L_c is the link distance between the typical cellular UE and the connected BS at the origin, L_i represents the link distance between the interfering cellular UE X_i and its associated BS, and $\|X_i\|$ is the distance between the interfering UE X_i and the BS located at the origin.[2]

2) D2D Mode: We model the D2D link length L_d using a Rayleigh distribution [18]

$$\begin{aligned} f_{L_d}(r) &= \frac{2\pi\lambda r}{\xi} \exp\left(-\frac{\pi\lambda r^2}{\xi}\right) \\ &= 2\pi\lambda' r \exp\left(-\lambda' \pi r^2\right), \\ \mathrm{P}\left(L_d \le r\right) &= 1 - \exp\left(-\lambda' \pi r^2\right), \quad r \ge 0, \end{aligned} \tag{6}$$

where $\lambda' = \frac{\lambda}{\xi}$ and ξ is a fitting parameter that affects the average D2D link distance. Specifically, the scale parameter

[2]Since each UE connects to the closest BS, the distance between an interfering UE and the BS at the origin is larger than the interfering UE's link distance, *i.e.*, $L_i \le \|X_i\|$. The interested reader is referred to [13] and [38] for a detailed description of (4) and (5). More discussions on the user distributions appear in [36].

of the Rayleigh distribution in (6) is $\sigma = \sqrt{\frac{\xi}{2\pi\lambda}}$ and the average D2D link distance is given by $\mathbb{E}[L_d] = \sigma\sqrt{\frac{\pi}{2}} = \sqrt{\frac{\xi}{4\lambda}}$, *i.e.*, $\xi = 4\lambda\mathbb{E}[L_d]^2$. D2D mode utilizes ALOHA with transmit probability ε on each time slot, where $0 \leq \varepsilon \leq 1$. Since the potential D2D UEs in D2D mode follow a location independent thinning process [18], the set of UEs operating in the D2D mode is distributed according to a homogeneous PPP Φ_d with intensity $\lambda_d = q\mathrm{P}(L_d \leq \theta)\lambda$, which is independent to the set of UEs in the cellular mode. Similarly, due to the location independent thinning induced by the ALOHA scheme, the set of active interfering UEs that gain access to the channel resource is distributed as a homogeneous PPP $\varepsilon\Phi_d$ with intensity $\varepsilon\lambda_d$, where $\varepsilon\Phi_d$ is a subset of Φ_d, *i.e.*, $\varepsilon\Phi_d \subset \Phi_d$.

Assumption 2: *In order to maintain tractability, we assume that $\varepsilon\Phi_d$ and $\hat{\Phi}_c$ are independent.*

C. Channel Inversion-Based Power Control

The received power at the origin from the UE X_i is $W = P_i\ \tau\|X_i\|^{-\alpha}\ G_i$, where P_i is the transmit power of the UE X_i, $\|X_i\|$ is the distance from X_i to the origin, α is the path-loss exponent, τ is the path-loss intercept at unit distance $\|X_i\| = 1$, and G_i represents the small-scale fading.[3] The coefficients $\{G_i\}$ of each link are assumed to be independent of one another.

We assume channel inversion based power control, *i.e.*, ${P_i} = {L_i}^{\alpha}$. Then, the received power is $W = \tau G_i\ (L_i/\|X_i\|)^{\alpha}$ for an interference link and $W = \tau G_i$ for the intended link. The transmit power of the UEs operating in the cellular mode $X_i \in \hat{\Phi}_c$ is $P_c = L_c^{\alpha}$, whereas that of the potential D2D UEs in the D2D mode $X_i \in \Phi_d$ is $P_d = L_d^{\alpha}$ given that $L_d \leq \theta$. Since a potential D2D UE may use either a D2D mode or a cellular mode, for the purpose of our calculations, its transmit power can be interpreted as the weighted average of the two operating mode events, *i.e.*, $\bar{P}_d = \mathrm{P}(L_d \leq \theta)P_d + \mathrm{P}(L_d > \theta)P_c$. Higher order moments of the transmit power for each mode are evaluated in the following lemma.

Lemma 1: *The l-th moments of the transmit power of a cellular UE (P_c), a potential D2D UE in D2D mode (P_d), and a potential D2D UE ($\bar{P}_d$) are respectively given by*

$$\begin{aligned}
\mathbb{E}\left[{P_c}^l\right] &= \frac{\Gamma\left(\frac{l}{\delta}+1\right)}{(\lambda_b\pi)^{\frac{l}{\delta}}},\\
\mathbb{E}\left[{P_d}^l\right] &= \frac{1}{(\lambda'\pi)^{\frac{l}{\delta}}}\left[\frac{\gamma\left(\frac{l}{\delta}+1, \lambda'\pi\theta^2\right)}{1-\exp\left(-\lambda'\pi\theta^2\right)}\right],\\
\mathbb{E}\left[\bar{P}_d^l\right] &= \frac{\exp\left(-\lambda'\pi\theta^2\right)}{(\lambda_b\pi)^{\frac{l}{\delta}}}\Gamma\left(\frac{l}{\delta}+1\right)\\
&\quad + \frac{1}{(\lambda'\pi)^{\frac{l}{\delta}}}\gamma\left(\frac{l}{\delta}+1, \lambda'\pi\theta^2\right),
\end{aligned} \tag{7}$$

where $\delta = \frac{2}{\alpha}$, $l > 0$ is a positive real-valued constant, $\lambda' = \frac{\lambda}{\xi}$, θ is the mode selection threshold, $\Gamma(t)$ is the gamma function, and $\gamma(s, x)$ is the lower incomplete gamma function (See Appendix I).

Proof: See Appendix II. □

Under this assumption, the received SINR for the two modes at the origin are given by

$$\begin{cases}
\mathrm{D2D}: \mathrm{SINR}_d = \dfrac{G_0}{\sum\limits_{X_j \in \varepsilon\Phi_d \setminus \{X_0\}} G_j L_j^{\alpha}\|X_j\|^{-\alpha} + N},\\
\mathrm{Cellular}: \mathrm{SINR}_c = \dfrac{G_0}{\sum\limits_{X_j \in \hat{\Phi}_c \setminus \{X_0\}} G_j L_j^{\alpha}\|X_j\|^{-\alpha} + N},
\end{cases} \tag{8}$$

where X_0 represents the typical UE, G_0 is the channel coefficient between the typical UE and the origin and $N = \frac{N_0}{\tau}$ is determined by the noise power spectral density N_0 and the reference path-loss τ at a unit distance.

TABLE II
SPECIAL CASES OF THE κ-μ AND η-μ FADING MODELS

	κ-μ	η-μ
Rayleigh	$\kappa \to 0, \mu = 1$	$\eta = 1, \mu = 0.5$
Rice	$\mu = 1$	
Nakagami-m	$\kappa \to 0, \mu = m$	$\eta = 1, \mu = m/2$ or $\eta \to 0, \mu = m$
Hoyt (Nakagami-q)		$\mu = 0.5$
One-sided Gaussian	$\kappa \to 0, \mu = 0.5$	$\eta \to 0, \mu = 0.5$ or $\eta \to \infty, \mu = 0.5$

III. THE κ-μ AND η-μ FADING MODELS

The physical channels of D2D networks are often characterized as inhomogeneous environments with clusters of scattered waves [22]. For example, strong line-of-sight (LOS) components, correlated in-phase and quadrature scattered waves with unequal-power, and non-circular symmetry are frequently observed in the physical channel of wireless networks [25]. Therefore, to evaluate the transmission performance over realistic channels, we adopt two very general fading distributions which together can model both homogeneous and inhomogeneous radio environments. These are:

1) The κ-μ Distribution: The κ-μ distribution represents the small-scale variation of the fading signal under LOS conditions, propagated through a homogeneous, linear, circularly symmetric environment [23]–[25]. The κ-μ distribution is a general fading distribution that includes Rayleigh, Rician, Nakagami-m, and One-sided Gaussian distributions as special cases (See Table II).

The received signal in a κ-μ fading channel consists of clusters of multipath waves, where the signal within each cluster has an elective dominant component and scattered waves with identical powers. The parameters κ and μ are related to the physical properties of the fading channel: κ represents the ratio between the total power of the dominant components and the total power of the scattered waves, whereas μ is the number of multipath clusters.[4]

[3]We have isolated and focused on studying the impact of the small scale fading upon the system model proposed here. Nonetheless, the model can be readily adapted to include shadowing by using the approach in [29, Lemma 1].

[4]Note that μ is initially assumed to be a natural number, however for the κ-μ fading model, this restriction is relaxed to allow μ to assume any positive real value.

The PDF, l-th moment and Laplace transform of G are respectively given by [23], [24], [41]

$$\begin{aligned} f_G(x) &= \frac{\mu\ x^{\frac{\mu-1}{2}}}{\kappa^{\frac{\mu-1}{2}}\ \mathrm{e}^{\mu\kappa}\ \Omega_{\kappa\mu}^{\frac{\mu+1}{2}}} \mathrm{e}^{-\frac{x}{\Omega_{\kappa\mu}}} \mathrm{I}_{\mu-1}\left(2\sqrt{\frac{\kappa\mu}{\Omega_{\kappa\mu}}x}\right), \\ \mathbb{E}\left[G^l\right] &= \frac{\Omega_{\kappa\mu}^l}{\mathrm{e}^{\mu\kappa}} \frac{\Gamma(\mu+l)}{\Gamma(\mu)} {}_1F_1(\mu+l;\mu;\mu\kappa), \\ \mathcal{L}_G(s) &= \mathbb{E}\left[\exp(-sG)\right] \\ &= \left(1+s\Omega_{\kappa\mu}\right)^{-\mu} \exp\left(-\frac{\mu\kappa}{1+\frac{1}{s\Omega_{\kappa\mu}}}\right), \end{aligned} \tag{9}$$

where $\bar{w} = \mathbb{E}[G]$, κ, μ and l are positive real values, $\Omega_{\kappa\mu} \triangleq \frac{\bar{w}}{\mu(1+\kappa)}$, $(x)_n = \frac{\Gamma(x+n)}{\Gamma(x)}$ represents the Pochhammer symbol, $\mathrm{I}_v(x)$ is the modified Bessel function of the first kind, and ${}_1F_1(a;b;x)$ is the confluent hypergeometric function.

2) The η-μ Distribution: The η-μ distribution is used to represent small scale fading under non-line-of-sight (NLOS) conditions in inhomogeneous, linear, non-circularly symmetric environments [23], [26]. It is a general fading distribution that includes Hoyt (Nakagami-q), One-sided Gaussian, Rayleigh, and Nakagami-m as special cases (See Table II).

The received signal in an η-μ fading channel is composed of clusters of multipath waves. The in-phase and quadrature components of the fading signal within each cluster are assumed to be either independent with unequal powers or correlated with identical powers. The parameter η denotes the scattered-wave power ratio between the in-phase and quadrature components and 2μ represents the real valued extension of the number of multipath clusters.

The PDF, l-th moment and Laplace transform of G are respectively given by [23], [24], [41]

$$\begin{aligned} f_G(x) &= \frac{2\sqrt{\pi}\,\mu^{\mu+\frac{1}{2}}h^{\mu}}{\Gamma(\mu)H^{\mu-\frac{1}{2}}\bar{w}^{\mu+\frac{1}{2}}} x^{\mu-\frac{1}{2}} \mathrm{e}^{-\frac{x}{\Omega_{\eta\mu}}} \mathrm{I}_{\mu-\frac{1}{2}}\left(\frac{x}{\Omega_{\eta\mu}}\right), \\ \mathbb{E}\left[G^l\right] &= \frac{\Omega_{\eta\mu}^l}{h^{\mu}} \frac{\Gamma(2\mu+l)}{\Gamma(2\mu)} \\ &\quad \times {}_2F_1\left(\mu+\frac{l}{2}+\frac{1}{2}, \mu+\frac{l}{2}; \mu+\frac{1}{2}; \left(\frac{H}{h}\right)^2\right), \\ \mathcal{L}_G(s) &= \frac{1}{h^{\mu}}\left[\left(1+s\Omega_{\eta\mu}\right)^2 - \left(\frac{H}{h}\right)^2\right]^{-\mu}, \end{aligned} \tag{10}$$

where $\bar{w} = \mathbb{E}[G]$, η, μ and l are positive real values,[5] $h = \frac{2+\eta^{-1}+\eta}{4}$, $H = \frac{\eta^{-1}-\eta}{4}$, $\Omega_{\eta\mu} \triangleq \frac{\bar{w}}{2\mu h}$ and ${}_2F_1(a,b;c;x)$ is the Gaussian hypergeometric function.

IV. Interference Model of the Overlay D2D Network

In this section, we introduce the interference of cellular and D2D links and derive the Laplace transform of the interference for the generalized fading channels considered here.

[5] h and H have two formats: format 1 is $h = \frac{2+\eta^{-1}+\eta}{4}$, $H = \frac{\eta^{-1}-\eta}{4}$ for $0 < \eta < \infty$, whereas format 2 is $h = \frac{1}{1-\eta^2}$, $H = \frac{\eta}{1-\eta^2}$ for $-1 < \eta < 1$. In this paper, we will only consider format 1 for notational simplicity.

A. D2D Mode

Let us consider a D2D link, where co-channel interference is generated by potential D2D UEs operating in D2D mode. Based on (8), the effective interference at the intended D2D receiver is

$$I_d = \sum_{X_j \in \varepsilon\Phi_d \setminus \{X_0\}} G_j L_j^{\alpha} \|X_j\|^{-\alpha}. \tag{11}$$

The point process Φ_d in (11) is similar to the D2D process in [18] since both models assume distance-based mode selection as well as Rayleigh distributed D2D link lengths. Nonetheless, the fading model in (11) affects the distribution of the aggregate interference and the corresponding distribution parameters, which is characterized by the Laplace transform of I_d as follows.

Lemma 2: *For overlay D2D, the Laplace transform of the interference at the D2D receiver is*

$$\mathcal{L}_{I_d}(s) = \exp\left(-c_d \cdot s^{\delta}\right), \tag{12}$$

where the constant terms c_d for the κ-μ and η-μ fading distributions are respectively given by

$$\begin{cases} \kappa-\mu: & \dfrac{c_0\Omega_{\kappa\mu}^{\delta}}{\mathrm{e}^{\mu\kappa}}\dbinom{\mu+\delta-1}{\delta} {}_1F_1(\mu+\delta;\mu;\mu\kappa), \\ \eta-\mu: & \dfrac{c_0\Omega_{\eta\mu}^{\delta}}{h^{\mu}}\dbinom{2\mu+\delta-1}{\delta} \\ & \quad \times {}_2F_1\left(\mu+\dfrac{\delta+1}{2}, \mu+\dfrac{\delta}{2}; \mu+\dfrac{1}{2}; \dfrac{H^2}{h^2}\right), \end{cases} \tag{13}$$

with $c_0 \triangleq \frac{q\varepsilon\xi}{\mathrm{sinc}(\delta)} \cdot \gamma\left(2, \lambda\pi\theta^2 \cdot \xi^{-1}\right)$, $\delta = \frac{2}{\alpha}$, $\bar{w} = \mathbb{E}[G]$, the fitting parameter ξ and ALOHA transmit probability ε.

Proof: See Appendix III. □

B. Cellular Mode

Based on Assumption 1, we model the interference at the cellular BS by a non-homogeneous PPP $\hat{\Phi}_c$ with intensity $\lambda_b\left(1-\exp\left(-\pi\lambda_b d^2\right)\right)$ [13], [38], where the interference in (8) is

$$I_c = \sum_{X_j \in \hat{\Phi}_c \setminus \{X_0\}} G_j L_j^{\alpha} \|X_j\|^{-\alpha}, \tag{14}$$

and the Laplace transform of I_c is evaluated as follows.

Lemma 3: *For overlay D2D, the Laplace transform of the interference at the cellular BS is*

$$\mathcal{L}_{I_c}(s) = \exp\left(-\mathcal{W}(s)\right), \tag{15}$$

where $\mathcal{W}(s)$ for each channel is respectively given by

$$\begin{aligned} \mathcal{W}(s) &= \frac{\mu \cdot s\ \Omega_{\kappa\mu}}{(1-\delta)\mathrm{e}^{\mu\kappa}} {}_2F_1(\mu+1, 1-\delta; 2-\delta; -s\Omega_{\kappa\mu}) \\ &\quad + \left(1+s\Omega_{\kappa\mu}\right)^{-\mu} \exp\left(-\mu\kappa \cdot \frac{s\Omega_{\kappa\mu}}{s\Omega_{\kappa\mu}+1}\right) - 1, \end{aligned} \tag{16}$$

for the κ-μ fading and

$$\begin{aligned} \mathcal{W}(s) &= \frac{2s\Omega_{\eta\mu}h^{\mu}}{(1-\delta)H^{2\mu}} \sum_{n=\mu}^{\infty} n \left(\frac{H}{h}\right)^{2n} \binom{n-1}{\mu-1} \\ &\quad \times {}_2F_1(1, 1-\delta-2n; 2-\delta; -s\Omega_{\eta\mu}) \\ &\quad + h^{-\mu}\left(\left(1+s\Omega_{\eta\mu}\right)^2 - \left(\frac{H}{h}\right)^2\right)^{-\mu} - 1, \end{aligned} \tag{17}$$

for the η-μ fading, $\delta = \frac{2}{\alpha}$, $\Omega_{\kappa\mu} \triangleq \frac{\bar{w}}{\mu(1+\kappa)}$ and $\Omega_{\eta\mu} \triangleq \frac{\bar{w}}{2\mu h}$.

Proof: See Appendix IV. □

Remark 1: *The Laplace transform of the interference in the cellular uplink is invariant to the node density λ_b. A similar behavior was observed in [38] for Rayleigh fading and Lemma 3 extends this invariance property to any fading model that can be represented by the κ-μ and η-μ distributions.*

Remark 2: *The invariance property and analytical tractability of Lemma 3 are special properties that only hold for the full channel-inversion based power control, i.e., $P_c = L_c^{\alpha}$. If we use fractional power control [13], [38], i.e., $P_c = L_c^{\alpha\epsilon}$ with $0 \leq \epsilon \leq 1$, then the Laplace transform of the aggregate interference depends on the BS density and the integral in (48) can not be easily partitioned into two single integral expressions, which significantly complicates the derivation.*

V. Stochastic Geometric Framework for System Performance Evaluation

To evaluate the network performance, one normally needs to calculate the average of some function of the SINR γ for a given SINR distribution $f_{\gamma}(x)$. The average of an arbitrary function of the SINR represents the most commonly used characteristics, such as the spectral efficiency, error probability, statistical moments, etc. Quite often this can be a challenging task because, within the stochastic geometry framework, a closed form expression for $f_{\gamma}(x)$ is known only for some special cases, such as Rayleigh [16] or Nakagami-*m* fading [31]. Instead, we can evaluate the Laplace transform of the interference $\mathcal{L}_I(s)$ using the PDF of the channel $f_G(x)$.

To this end, we exploit a novel method to evaluate the average of an arbitrary function of the SINR by using $\mathcal{L}_I(s)$ and $f_G(x)$ only, without $f_{\gamma}(x)$. The original idea was proposed by Hamdi [42] for Nakagami-*m* fading and was utilized in [43] to evaluate the network performance over composite Nakagami-*m* fading and Log-Normal shadowing channels, composite Rice fading and Log-Normal shadowing channels and correlated Log-Normal shadowing. In this paper, we apply Hamdi's approach to κ-μ and η-μ fading, thereby extending the applicability to the majority of the fading models known in the literature.

Theorem 1: *The average $\mathbb{E}\left[g\left(\frac{G_0}{I+N}\right)\right]$ of an analytic function $g(x)$ can be evaluated as follows*

$$\mathbb{E}\left[g\left(\frac{G_0}{I+N}\right)\right] = g(0) + \sum_{n=0}^{\infty} \frac{(\mu\kappa)^n}{n!\ \mathrm{e}^{\mu\kappa}} \varphi_{\kappa\mu}(n), \tag{18}$$

for the κ-μ distributed signal envelope, where κ, μ, η are non-negative real valued constants, $\varphi_{\kappa\mu}(n)$ and $g_i(z)$ represent the following expressions

$$\begin{aligned} \varphi_{\kappa\mu}(n) &\triangleq \int_0^{\infty} g_{\mu+n}(z)\, \mathcal{L}_I\left(\frac{z}{\Omega_{\kappa\mu}}\right) \exp\left(-\frac{Nz}{\Omega_{\kappa\mu}}\right) \mathrm{d}z, \\ g_i(z) &= \frac{1}{\Gamma(\mu+n)} \frac{\mathrm{d}^i}{\mathrm{d}z^i}\left(z^{\mu+n-1} g(z)\right). \end{aligned} \tag{19}$$

Similarly, for the η-μ faded signal envelope,

$$\begin{aligned} \mathbb{E}\left[g\left(\frac{G_0}{I+N}\right)\right] &= g(0) + \sum_{n=0}^{\infty} a_n \varphi_{\eta\mu}(n), \\ a_n &= \binom{n+\mu-1}{n} \frac{(H/h)^{2n}}{h^{\mu}}, \end{aligned} \tag{20}$$

where $\varphi_{\eta\mu}(n)$ and $g_i(z)$ denote the following expressions

$$\begin{aligned} \varphi_{\eta\mu}(n) &\triangleq \int_0^{\infty} g_{2\mu+2n}(z)\, \mathcal{L}_I\left(\frac{z}{\Omega_{\eta\mu}}\right) \exp\left(-\frac{Nz}{\Omega_{\eta\mu}}\right) \mathrm{d}z, \\ g_i(z) &= \frac{1}{\Gamma(2\mu+2n)} \frac{\mathrm{d}^i}{\mathrm{d}z^i}\left(z^{2\mu+2n-1} g(z)\right). \end{aligned} \tag{21}$$

Proof: See Appendix V. □

Theorem 1 provides a general framework to evaluate arbitrary system performance measures when the received signal power G_0 follows either a Gamma distribution or a mixture of Gamma distributions, which includes κ-μ and η-μ and the majority of the most popular linear fading models utilized in the literature.[6] We note that Theorem 1 makes no assumption on the underlying distribution of the constituent interference channels. Therefore it can be applied even when the intended signal and interfering links are described by different fading models.

In the following, we apply Theorem 1 and Lemmas 1-3 to evaluate various performance measures for overlaid D2D networks.

A. Spectral Efficiency

The spectral efficiency R of an overlaid D2D network is determined in part by the amount of accessible radio resources, denoted by $\triangle$, to each operating mode as follows

$$R = \triangle \cdot \mathbb{E}\left[\log\left(1 + \frac{G_0}{I+N}\right)\right]. \tag{22}$$

In D2D mode, due to the ALOHA medium access, ε percent of the transmitting UEs will gain access to the spectrum resource for the D2D transmission, which is β fraction of the available spectrum. In cellular mode, $1-\beta$ fraction of the available spectrum is allocated to the cellular transmission and only one uplink transmitter within each cell can stay active at any given resource block due to the orthogonal multiple access. Thereby, the amount of accessible spectrum resource is $\triangle_d = \beta\varepsilon$ for the D2D transmission and $\triangle_c = (1-\beta)\mathbb{E}\left[\frac{1}{M}\right]$ for the cellular transmission, where M is the number of potential cellular UEs within a cell. The average $\mathbb{E}\left[\frac{1}{M}\right]$ is evaluated in [18] as $\mathbb{E}\left[\frac{1}{M}\right] = \frac{\lambda_b}{\lambda_c}\left(1 - \mathrm{e}^{-\frac{\lambda_c}{\lambda_b}}\right)$ where $\lambda_c = [(1-q) + q\mathrm{P}(L_d > \theta)]\,\lambda$.

Since a potential D2D UE may choose either cellular or D2D mode, the spectral efficiency of an arbitrary potential D2D UE is the average of the two operating modes. By using Theorem 1 and Lemmas 2, 3, the average term $\mathbb{E}\left[\log\left(1+\frac{G_0}{I+N}\right)\right]$ in (22) can be calculated and the spectral

[6] The interested reader is referred to [44] for a detailed description of the fading models that can be represented as a mixture of Gamma distributions.

efficiency of the D2D and cellular modes can be evaluated as follows.

Theorem 2: *For an overlaid D2D network, the spectral efficiency of a cellular UE (R_c), a potential D2D UE operating in D2D modes (R_d), and a potential D2D UE ($\bar{R}_d$) are given by*

$$\begin{aligned} R_c &= \frac{(1-\beta)\left(1-\mathrm{e}^{-\frac{\lambda_c}{\lambda_b}}\right)\lambda_b}{\lambda_c}\mathbb{E}\left[\log\left(1+\frac{G_0}{I_c+N}\right)\right], \\ R_d &= \beta\varepsilon\mathbb{E}\left[\log\left(1+\frac{G_0}{I_d+N}\right)\right], \\ \bar{R}_d &= \mathrm{P}\left(L_d>\theta\right)R_c+\mathrm{P}\left(L_d\le\theta\right)R_d, \end{aligned} \tag{23}$$

where β is the spectrum partition factor, ε is the ALOHA transmit probability, ξ is a fitting parameter for the D2D link length distribution and $\mathrm{P}\left(L_d\le\theta\right)=1-\exp\left(-\lambda\pi\theta^2\cdot\xi^{-1}\right)$ from (6). The average term $\mathbb{E}\left[\log\left(1+\frac{G_0}{I+N}\right)\right]$ can be evaluated using Theorem 1 as follows

$$\mathbb{E}\left[\log\left(1+\gamma\right)\right]=\begin{cases}\dfrac{1}{\mathrm{e}^{\mu\kappa}}\displaystyle\sum_{n=0}^{\infty}\frac{(\mu\kappa)^n}{n!}\varphi_{\kappa\mu}(n) & \text{for } \kappa-\mu\\ \displaystyle\sum_{n=0}^{\infty}a_n\varphi_{\eta\mu}(n) & \text{for } \eta-\mu\end{cases} \tag{24}$$

where a_n is defined in (21), $\varphi_{\kappa\mu}(n)$ and $\varphi_{\eta\mu}(n)$ are defined in Theorem 1, $\mathcal{L}_I(s)$ is given by (12) for the D2D mode and (15) for the cellular mode. The derivative terms $g_i(x)$ for the logarithm function $g(x)=\log(1+\mathrm{SINR})$ is evaluated in [42] as $g_i(x)=\frac{1}{x}\left(1-\frac{1}{(1+x)^i}\right)$.

Remark 3: *We observe that R_c in (23) is a decreasing function of the spectrum partition factor β, whereas R_d and $\bar{R}_d$ are increasing functions of β. For a UE operating in cellular mode, R_c is an increasing function of the mode selection threshold θ: Given a large θ, more UEs will choose the D2D mode and the average number of the cellular UEs in a cell $\mathbb{E}[N]$ will decrease. On the other hand, R_d is a decreasing function of θ due to the increased D2D interference. Since $\bar{R}_d$ is the average of R_c and R_d, $\bar{R}_d$ is concave function of θ. (See Section VI)*

Remark 4: *Theorem 2 can be applied to the general case when different types of fading affect the intended and interfering links. For example, if the fading observed in the intended link is κ-μ distributed and that of the interference link is η-μ distributed, then the average of the logarithm function can be evaluated using (24) where the Laplace transform of the interference $\mathcal{L}_I(s)$ is given by (12) and (13) for the D2D mode (or (15) and (17) for the cellular mode).*

Remark 5: *Theorem 1 can be utilized to evaluate any performance measures that are represented as a function of SINR. The analytic function $g(x)$ and the corresponding $g_i(x)$ for several performance measures are summarized in Table III,*[7] *where one can substitute $i=\mu+n$ to $g_i(x)$ for the κ-μ distribution and $i=2\mu+2n$ for the η-μ distribution.*

[7]The detailed proof of Table III is given in [42].

TABLE III
DIFFERENT $g(x)$ AND $g_i(x)$ FOR EVALUATING VARIOUS SYSTEM MEASURES

Measure	$g(x)$	$g_i(x)=\frac{1}{\Gamma(i)}\frac{\mathrm{d}^i}{\mathrm{d}x^i}x^{i-1}g(x)$
Spectral efficiency	$\log(1+x)$	$\frac{1}{x}\left(1-\frac{1}{(1+x)^i}\right)$
Error bound	e^{-x}	$-i_1F_1(1-i;2;x)\mathrm{e}^{-x}$
Higher order moments	x^r	$\frac{\Gamma(i+r)}{\Gamma(i)\Gamma(r)}x^{r-1}$

B. Outage Probability

The outage probability is defined for the D2D and cellular mode as follows

$$P_o(T_o)=\begin{cases}\mathbb{P}\left(\dfrac{G_0}{I_d+N}<T_o\right) & \text{for D2D mode,}\\ \mathbb{P}\left(\dfrac{G_0}{I_c+N}<T_o\right) & \text{for Cellular mode,}\end{cases} \tag{25}$$

with a predefined SINR threshold T_o. Although Theorem 1 presents a generalized framework to calculate any performance measure that is represented as an analytic function of the SINR, it can not be used for evaluating SINR distribution based performance measures, such as the outage probability or rate coverage probability. For the outage probability, $g(x)=\mathbb{I}(x<T_0)$ is a step function and its higher order derivative is an unbounded impulse signal.

Instead of using Theorem 1, we use the series representation of the κ-μ and η-μ fading distributions and employ Campbell's theorem [12], [14] to represent the SINR distribution in terms of the Laplace transform of the aggregate interference as follows. The SINR distributions $\mathbb{P}\left(\mathrm{SINR}<T_o\right)$ in (25) can be evaluated as

$$\begin{aligned}&\sum_{n=0}^{\infty}\sum_{m=0}^{\infty}b_{n,m}^{\kappa\mu}\mathbb{E}\left[\left(\frac{T_o\left(I+N\right)}{\Omega}\right)^{n+\mu+m}\mathrm{e}^{-\frac{T_o(I+N)}{\Omega}}\right]\\ &\quad=\sum_{n=0}^{\infty}\sum_{m=0}^{\infty}b_{n,m}^{\kappa\mu}\mathbb{E}_t\left[t^{n+\mu+m}\mathrm{e}^{-t}\right],\end{aligned} \tag{26}$$

for κ-μ fading, where we applied (60) with $\frac{T_o(I+N)}{\Omega}=t$, $\Omega_{\kappa\mu}=\frac{\bar{w}}{\mu(1+\kappa)}$ and $b_{n,m}^{\kappa\mu}=\frac{(\mu\kappa)^n\mathrm{e}^{-\mu\kappa}}{n!\cdot\Gamma(n+\mu+m+1)}$. The term $\mathbb{E}_t\left[t^n\mathrm{e}^{-t}\right]$ in (26) can be evaluated as follows

$$\begin{aligned}\mathbb{E}_t\left[t^n\mathrm{e}^{-t}\right]&=(-1)^n\left.\frac{\partial^n\mathcal{L}_t(s)}{\partial s^n}\right|_{s=1},\\ \mathcal{L}_t(s)&=\mathbb{E}\left[\mathrm{e}^{-s\frac{T_o(I+N)}{\Omega}}\right]=\mathrm{e}^{-\frac{sT_oN}{\Omega}}\mathcal{L}_I\left(\frac{sT_o}{\Omega}\right),\end{aligned} \tag{27}$$

where $\mathcal{L}_I(s)$ is derived in Lemma 2 for the D2D link and Lemma 3 for the cellular link. Therefore, the outage probability of an overlaid D2D network is derived as follows

$$\begin{aligned}&\mathbb{P}\left(\mathrm{SINR}<T_o\right)\\ &=\begin{cases}\displaystyle\sum_{n=0}^{\infty}\sum_{m=0}^{\infty}b_{n,m}^{\kappa\mu}\mathcal{K}^{(n+m+\mu)}(T_o) & \text{for } \kappa-\mu,\\ \displaystyle\sum_{n=0}^{\infty}\sum_{m=0}^{\infty}b_{n,m}^{\eta\mu}\mathcal{K}^{(2n+2\mu+m)}(T_o) & \text{for } \eta-\mu,\end{cases}\end{aligned} \tag{28}$$

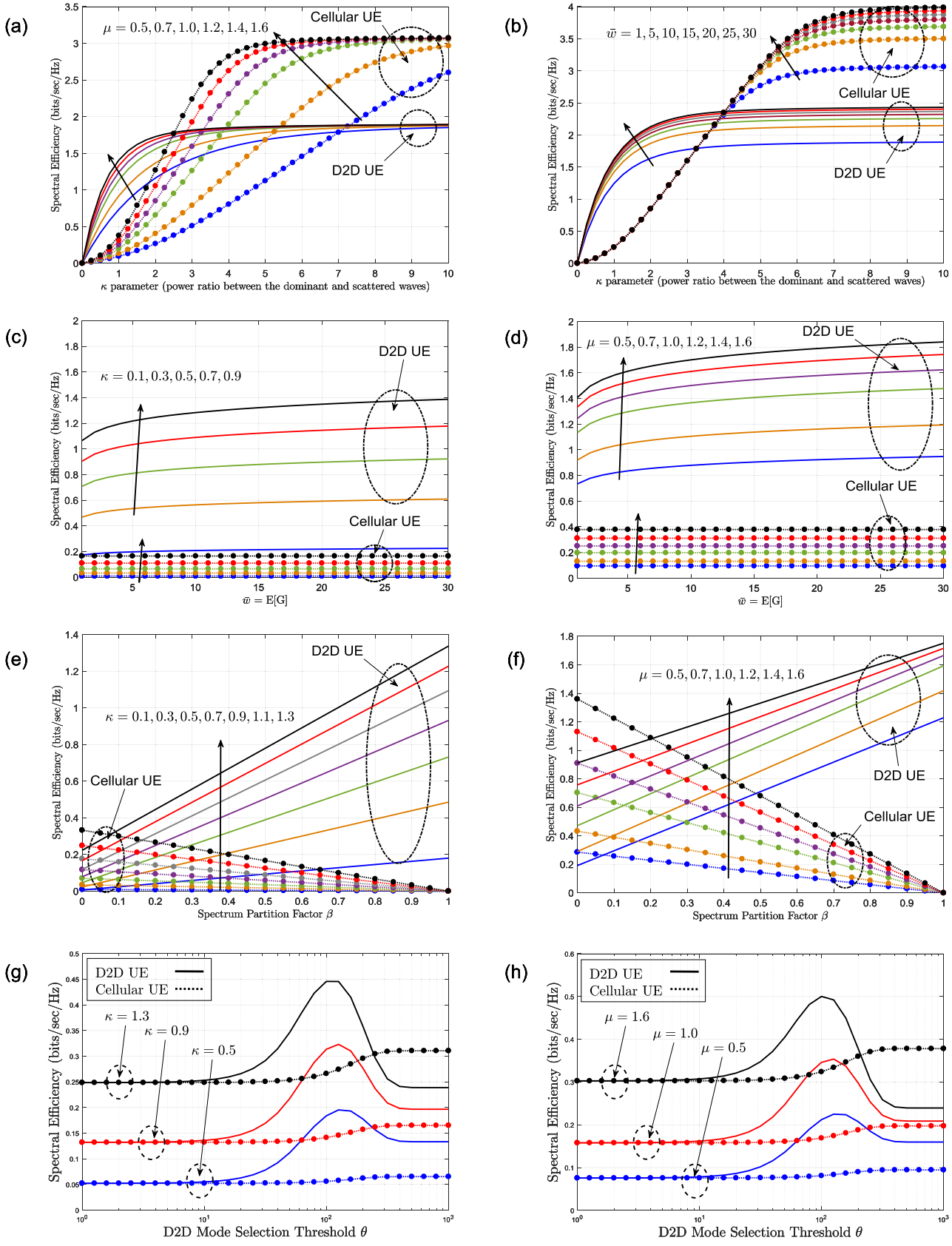

Fig. 2. Spectral efficiency of an overlaid D2D network for various channel parameters $(\kappa, \mu, \bar{w})$; (a)-(h) assume $\lambda_b = \frac{1}{\pi 500^2}$, $\lambda = 10\lambda_b$, $\varepsilon = 0.8$, $\alpha = 4$, $\beta = 0.2$, $\theta = 100m$, $q = 0.2$ and $N = \frac{N_0}{\tau} = -60$ (dBm/Hz).

where (61) is used for the η-μ fading and $\mathcal{K}^{(l)}(T_o)$ denotes the higher order derivative terms as

$$\mathcal{K}^{(l)}(T_o) = (-1)^l \frac{\partial^l}{\partial s^l}\left[\mathrm{e}^{-\frac{sT_oN}{\Omega}}\mathcal{L}_I\left(\frac{sT_o}{\Omega}\right)\right]\Bigg|_{s=1}. \quad (29)$$

The outage probability of the D2D mode (or cellular mode) can be evaluated by substituting $\mathcal{L}_{I_d}(s)$ from Lemma 2 (or $\mathcal{L}_{I_c}(s)$ from Lemma 3) into (29). The higher order derivative in (29) can be numerically evaluated by using Faa di Bruno's formula [45], as used in some related studies [31], [46].

VI. Numerical Results

In the following, we compare numerical results for different fading models. All of the simulations were carried out using MATLAB with the following parameters: BS node intensity $\lambda_b = \frac{1}{\pi 500^2}$, UE node intensity $\lambda = \frac{10}{\pi 500^2}$, ALOHA transmit probability $\varepsilon = 0.8$, path-loss exponent $\alpha = 4$, spectrum partition factor $\beta = 0.2$, mode selection threshold $\theta = 100m$, probability of potential D2D UEs $q = 0.2$, and effective noise $N = \frac{N_0}{\tau} = -60$ (dBm/Hz), where N_0 is the noise spectral density and τ is the reference path-loss at a unit distance. Without loss of generality, we assume identical fading parameters across the intended and interference links.

We have assumed $\xi = \lambda$ in Figs 2(a)-(d) and respectively used $\bar{\omega} = 1$ for Fig. 2(a), $\mu = 1.2$ for Fig. 2(b), $\mu = 1$ for Fig. 2(c) and $\kappa = 1$ for Fig. 2(d). We observe that a dominant LOS component (large κ), a large number of scattering clusters (large μ) and higher average of the channel coefficients (large $\bar{\omega}$) collectively achieve a higher spectral efficiency. In a weak LOS condition, the D2D links achieve higher spectral efficiency than the cellular links because, on average, D2D links have a closer transmission range than cellular links. In a strong LOS condition, the cellular links achieve higher spectral efficiency than the D2D links. In this case, the rate performance of the D2D link deteriorates due to the increased interference power from closely located D2D UEs. On the other hand, cellular links employ orthogonal medium access to ensure only one active transmitter within the cell at a given resource block. The received signal of the cellular links is protected against the elevated interference power, achieving higher cellular rate than the D2D links. We also note that the spectral efficiency is an increasing function of $\bar{\omega}$. Here, the rate increment of the D2D link is notable over the whole range of κ, whereas the increment of cellular link is distinguishable only after $\kappa \geq 5$.

In Figs 2(e)-(h), we have assumed $\xi = 1$ and $\bar{\omega} = 1$ and used $\mu = 1$ for Fig. 2(e), $\kappa = 2$ for Fig. 2(f), $\mu = 1$ for Fig. 2(g) and $\kappa = 1$ for Fig. 2(h), respectively. Since the spectral efficiency of a cellular UE R_c is a decreasing function of the spectrum partition factor β (and $\bar{R}_d$ is an increasing function of β), there is a crossover point β^* between the spectral efficiencies of the D2D and cellular link, which depends on the fading parameters. On average, D2D links have a closer transmission range than cellular links, hence if a minimum amount of spectrum is allocated to the D2D link, which is $\beta \geq \beta^*$, D2D UEs achieve higher transmission rates than cellular UEs. On the other hand, if $\beta < \beta^*$, D2D transmission does not have enough radio resources to achieve rate gains against the cellular link. As the number of scattering clusters increases, the spectral efficiency of the cellular UE becomes larger than that of the D2D UE and the crossover point β^* shifts towards the right.

Figs 2(g)-(h) show the effect of the mode selection threshold θ on the spectral efficiency for κ-μ fading. As shown in the figure, increasing θ results in less potential D2D UEs choosing to operate in the cellular mode, leading to a higher average rate for the cellular link. The spectral efficiency of a potential D2D UE in D2D mode R_d is a decreasing function of θ due to the increased co-channel interference over the D2D link. Since the spectral efficiency of a potential D2D UE $\bar{R}_d$ is a weighted average of R_c and R_d, $\bar{R}_d$ is concave function of θ as indicated in Figs 2(g)-(h).

VII. Conclusion

In this paper, we have considered a D2D network overlaid on an uplink cellular network, where the locations of the mobile UEs as well as the BSs are modeled as PPP. In particular, we exploited a novel stochastic geometric approach for evaluating the D2D network performance under the assumption of generalized fading conditions described by the κ-μ and η-μ fading models. Using these methods, we evaluated the spectral efficiency and outage probability of the overlaid D2D network. Specifically, we observed that the D2D link provides higher rates than those of the cellular link when the spectrum partition factor was appropriately chosen. Under these circumstances, setting a large mode selection threshold will encourage more UEs to use the D2D mode, which increases the average rate at the cost of a higher level of interference and degraded outage probability. However, for smaller values of the spectrum partition factor, the D2D link has smaller rates than those of the cellular link. In terms of the fading parameters, a dominant LOS component (large κ) or a large number of scattering clusters (large μ) improve the network performance, *i.e.*, a higher rate and lower outage probability are achieved. Finally, we also provided numerical results to demonstrate the performance gains of overlaid D2D networks compared to traditional cellular networks, where the latter corresponds to the $\beta = 0$ case.

Appendix I

For conciseness, in this appendix, we summarize the operational equalities of some special functions, which are used in this paper.[8] The following properties hold for non-negative real constants x and y

$$\Gamma(x)\Gamma\left(x+\frac{1}{2}\right) = 2^{1-2x}\sqrt{\pi}\Gamma(2x),$$
$$\binom{x}{y} = \frac{\Gamma(x+1)}{\Gamma(y+1)\Gamma(x-y+1)},$$
$$\Gamma(1+x)\Gamma(1-x) = \frac{1}{\mathrm{sinc}(x)}, \quad \Gamma\left(\frac{1}{2}\right) = \sqrt{\pi}. \quad (30)$$

[8]Most of the expressions in Appendix I were introduced in [47], except for (38) and (39), which were proved in [48].

The following properties of the hypergeometric function hold for real constants a, b and c

$$
\begin{aligned}
&{}_1F_1(a;b;t) = \mathrm{e}^t\,{}_1F_1(b-a;b;-t),\\
&{}_2F_1(a,b;c;z) = (1-z)^{-a}\,{}_2F_1\left(a,c-b;c;\frac{z}{z-1}\right), \qquad (31)\\
&\int_0^\infty \frac{t^{\alpha-1}}{\mathrm{e}^{ct}}\,{}_1F_1(a;b;-t)\mathrm{d}t = \frac{\Gamma(\alpha)}{c^\alpha}\,{}_2F_1\left(a,\alpha;b;-\frac{1}{c}\right), \qquad (32)\\
&((a-b)z+c-2a)\,{}_2F_1(a,b;c;z)\\
&= (c-a)\,{}_2F_1(a-1,b;c;z) + a\,(z-1)\,{}_2F_1(a+1,b;c;z), \qquad (33)\\
&\int_0^\infty x^{d-1}\mathrm{e}^{-bx}\gamma\,(c,ax)\,\mathrm{d}x\\
&= \frac{a^c\Gamma(d+c)}{c(a+b)^{d+c}}\,{}_2F_1\left(1,d+c;c+1;\frac{a}{a+b}\right), \qquad (34)
\end{aligned}
$$

where (32) holds for $\alpha > 0$ and $c > 0$, (34) holds for $a+b > 0$, $b > 0$, and $c + d > 0$. The modified Bessel function $\mathrm{I}_\nu(x)$ and incomplete gamma function $\gamma(s,x) = \int_0^x t^{s-1}\mathrm{e}^{-t}\mathrm{d}t$ can be represented by the hypergeometric function with arbitrary positive real constants ν, s, b as follows

$$
\begin{aligned}
\mathrm{I}_{\nu-1}(2\sqrt{bt}) &= \frac{{}_0F_1(;\nu;bt)}{\Gamma(\nu)}\,(bt)^{\frac{\nu-1}{2}},\\
\gamma(s,x) &= s^{-1}x^s\mathrm{e}^{-x}\,{}_1F_1(1;1+s;x),
\end{aligned} \qquad (35)
$$

where

$$
\begin{aligned}
\mathrm{I}_\nu(x) &= \sum_{n=0}^\infty \frac{1}{n!\,\Gamma(n+\nu+1)}\left(\frac{x}{2}\right)^{2n+\nu},\\
\frac{\gamma(s,x)}{\Gamma(s)} &= \sum_{n=0}^\infty \frac{x^{s+n}\mathrm{e}^{-x}}{\Gamma(s+n+1)},
\end{aligned} \qquad (36)
$$

$$
{}_0F_1(;\nu;bt) = \lim_{a\to\infty}\,{}_1F_1\left(a;\nu;\frac{bt}{a}\right). \qquad (37)
$$

Appell's function $F_2(\cdot)$ is defined via the Pochhammer symbol $(x)_n = \frac{\Gamma(x+n)}{\Gamma(x)}$ as follows

$$
F_2\left(\alpha;\beta,\beta';\gamma,\gamma';x,y\right) = \sum_{m=0}^\infty\sum_{n=0}^\infty \frac{(\alpha)_{m+n}\,(\beta)_m\,(\beta')_n}{m!\,n!\,(\gamma)_m\,(\gamma')_n}x^m y^n. \qquad (38)
$$

Appell's function can be reduced to the hypergeometric function using the following properties

$$
\begin{aligned}
F_2\left(d;a,a';c,c';0,y\right) &= {}_2F_1(d,a';c';y),\\
F_2\left(d;a,a';c,c';x,0\right) &= {}_2F_1(d,a;c;x).
\end{aligned} \qquad (39)
$$

The following integration holds under the following constraints $d > 0$ and $|k| + |k|' < |h|$

$$
\begin{aligned}
&\int_0^\infty t^{d-1}\mathrm{e}^{-ht}\,{}_1F_1(a;b;kt)\,{}_1F_1(a';b';k't)\mathrm{d}t\\
&= h^{-d}\Gamma(d)F_2\left(d;a,a';b,b';\frac{k}{h},\frac{k'}{h}\right).
\end{aligned} \qquad (40)
$$

Gaussian-Laguerre quadratures can be used to evaluate the integral for a given analytic function $g(x)$ as

$$
\int_0^\infty \mathrm{e}^{-x}g(x)\mathrm{d}x = \sum_{n=1}^N w_n f\,(x_n) + R_N, \qquad (41)
$$

where x_n and w_n are the n-th abscissa and weight of the N-th order Laguerre polynomial, respectively. The remainder R_N rapidly converges to zero [47].

APPENDIX II

In this appendix, we provide a proof for Lemma 1. First, the transmit power of a cellular UE is $P_c = {L_c}^\alpha$ and the pdf of L_c is given by (4). Then, the l-th moment of P_c is given by

$$
\begin{aligned}
\mathbb{E}\left[{P_c}^l\right] &= \int_0^\infty \left(x^\alpha\right)^l f_{L_c}(x)\mathrm{d}x\\
&= 2\pi\lambda_b\int_0^\infty x^{\alpha l+1}\exp\left(-\lambda_b\pi x^2\right)\mathrm{d}x\\
&= (\lambda_b\pi)^{-\frac{l}{\delta}}\,\Gamma\left(\frac{l}{\delta}+1\right),
\end{aligned} \qquad (42)
$$

where we applied a change of variable, *i.e.*, $\lambda_b\pi x^2 = t$, and used the notion of the gamma function $\Gamma(t) = \int_0^\infty x^{t-1}\mathrm{e}^{-x}\mathrm{d}x$ in the last equality. Similarly, the transmit power of D2D mode is $P_d = {L_d}^\alpha$, given that the criterion $L_d \le \theta$ is met. Then, the l-th moment of P_d is given by

$$
\begin{aligned}
\mathbb{E}\left[{P_d}^l\right] &= \mathbb{E}\left[{L_d}^{\alpha l}|L_d \le \theta\right] = \int_0^\theta x^{\alpha l}\frac{f_{L_d}(x)}{\mathrm{P}\,(L_d\le\theta)}\mathrm{d}x\\
&= \frac{2\pi\lambda'}{1-\mathrm{e}^{-\lambda'\pi\theta^2}}\int_0^\theta x^{\alpha l+1}\exp\left(-\lambda'\pi x^2\right)\mathrm{d}x\\
&= \frac{1}{(\lambda'\pi)^{\frac{l}{\delta}}}\left[\frac{\gamma\,\left(\frac{l}{\delta}+1,\lambda'\pi\theta^2\right)}{1-\mathrm{e}^{-\lambda'\pi\theta^2}}\right],
\end{aligned} \qquad (43)
$$

where we substituted (6) in the second equality, applied a change of variable, *i.e.*, $\lambda'\pi x^2 = t$, and used the notion of the lower incomplete gamma function $\gamma(s,x) = \int_0^x t^{s-1}\mathrm{e}^{-t}\mathrm{d}t$ with $\lambda' = \frac{\lambda}{\xi}$ in the last equality. Since a potential D2D UE may choose either cellular or D2D mode, the average transmit power of an arbitrary potential D2D UE is the average of the two operating modes as follows

$$
\mathbb{E}\left[\bar{P}_d^l\right] = \mathrm{P}(L_d\le\theta)\mathbb{E}\left[{P_d}^l\right] + \mathrm{P}(L_d>\theta)\mathbb{E}\left[{P_c}^l\right]. \qquad (44)
$$

where we obtain (7) by substituting (42) and (43) in (44). This completes the proof.

APPENDIX III

In this appendix, we provide a proof for Lemma 2. The Laplace transform of the interference at the D2D receiver $\mathcal{L}_{I_d}(s)$ is evaluated as follows

$$
\exp\left(-2\pi\varepsilon\lambda_d\int_0^\infty\left(1-\mathbb{E}\left[\exp\left(-sGL_d^\alpha\,r^{-\alpha}\right)\right]\right)r\mathrm{d}r\right), \qquad (45)
$$

where we considered the location independent thinning by ALOHA transmit probability ε and used the probability generating functional (PGFL) of PPP [12]. Then, by applying a change of variable, *i.e.*, $sGL_d^\alpha r^{-\alpha} = t$, and integration by parts, the Laplace transform $\mathcal{L}_{I_d}(s)$ simplifies as

$$
\begin{aligned}
&\exp\left(-\pi\varepsilon\lambda_d\mathbb{E}\left[(sG)^\delta L_d^2\int_0^\infty\delta t^{-\delta-1}\left(1-\mathrm{e}^{-t}\right)\mathrm{d}t\right]\right)\\
&= \exp\left(-\pi\varepsilon\lambda_d s^\delta\Gamma\,(1-\delta)\,\mathbb{E}\left[L_d^2\right]\mathbb{E}\left[G^\delta\right]\right),
\end{aligned} \qquad (46)
$$

where we used the gamma function $\Gamma(t) = \int_0^\infty x^{t-1}\mathrm{e}^{-x}\mathrm{d}x$ in the last equality. Hence, (13) for κ-μ fading can be obtained by substituting $\lambda_d = q\mathrm{P}(L_d \le \theta)\lambda$, (7), (9) into (46) as follows

$$\begin{aligned} c_d &= \pi\varepsilon\lambda_d\Gamma(1-\delta)\,\mathbb{E}\left[L_d^2\right]\mathbb{E}\left[G^\delta\right] \\ &= \frac{q\varepsilon\xi}{\mathrm{sinc}(\delta)}\cdot\frac{\gamma\left(2,\lambda\pi\theta^2\cdot\xi^{-1}\right){}_1F_1(\mu+\delta;\mu;\mu\kappa)}{\mathrm{e}^{\mu\kappa}} \\ &\quad\times\left(\frac{\bar{w}}{(1+\kappa)\mu}\right)^\delta\binom{\mu+\delta-1}{\delta}, \end{aligned} \tag{47}$$

where we used (30) in the last equality. Similarly, the Laplace transform of I_d for the η-μ distribution can be evaluated by using (10). This completes the proof.

Appendix IV

In this appendix, we provide a proof for Lemma 3. The Laplace transform of the interference at the cellular BS $\mathcal{L}_{I_c}(s)$ is evaluated as follows [13], [38]

$$\mathcal{L}_{I_c}(s) = \exp\left(-2\pi\lambda_b\phi(s)\right), \tag{48}$$

where $\phi(s)$ is defined as follows

$$\begin{aligned} \phi(s) &= \int_0^\infty\left(1-\mathrm{e}^{-\pi\lambda_b x^2}\right)\mathbb{E}\left[1-\mathrm{e}^{-sGL_j^a x^{-\alpha}}\right]x\mathrm{d}x \\ &= \int_0^\infty\int_0^x r\mathrm{e}^{-\pi\lambda_b r^2}\mathbb{E}\left[1-\mathrm{e}^{-sGr^\alpha x^{-\alpha}}\right]\mathrm{d}r\cdot x\mathrm{d}x \\ &= \int_0^\infty r\mathrm{e}^{-\pi\lambda_b r^2}\int_r^\infty x\cdot\mathbb{E}\left[1-\mathrm{e}^{-sGr^\alpha x^{-\alpha}}\right]\mathrm{d}x\ \mathrm{d}r \\ &= I_1\cdot I_2, \end{aligned} \tag{49}$$

where the PGFL of non-homogeneous PPP with intensity function $\lambda_b\left(1-\exp\left(-\pi\lambda_b d^2\right)\right)$ is used in the first equality, (5) is applied in the second equality, Fubini's theorem [49] is utilized to change the order of integration in the third equality and a change of variable, *i.e.*, $(r/x)^2 = t$, is used in the last equality. I_1 and I_2 in (49) represent the following integrals

$$\begin{aligned} I_1 &\triangleq \int_0^\infty r^3\exp\left(-\pi\lambda_b r^2\right)\mathrm{d}r, \\ I_2 &\triangleq \mathbb{E}_G\left\{\int_0^1 t^{-2}\left(1-\exp\left(-sGt^{\frac{1}{\delta}}\right)\right)\mathrm{d}t\right\}, \end{aligned} \tag{50}$$

which convert the double integral into a multiplication of two single integrals that are independent to each other.

The first integral I_1 in (49) can be evaluated by using a change of variable, *i.e.*, $\pi\lambda_b r^2 = t$, and the definition of the gamma function $\Gamma(t) = \int_0^\infty x^{t-1}\mathrm{e}^{-x}\mathrm{d}x$ as follows

$$I_1 = \frac{1}{2(\pi\lambda_b)^2}\int_0^\infty t\exp(-t)\,\mathrm{d}t = \frac{\Gamma(2)}{2(\pi\lambda_b)^2} = \frac{1}{2(\pi\lambda_b)^2}. \tag{51}$$

The second integral I_2 can be simplified by using a change of variable, *i.e.*, $sGt^{\frac{1}{\delta}} = u$, integration by parts and the definition of the lower incomplete gamma function $\gamma(s,x)$ as follows

$$\begin{aligned} I_2 &= \mathbb{E}_G\left\{(sG)^\delta\int_0^{sG}\delta u^{-\delta-1}\left(1-\exp(-u)\right)\mathrm{d}u\right\} \\ &= \mathbb{E}_G\left\{(sG)^\delta\gamma(1-\delta,sG)-\left(1-\exp(-sG)\right)\right\} \\ &= I_3+\mathcal{L}_G(s)-1, \end{aligned} \tag{52}$$

where $\mathcal{L}_G(s)$ represents the Laplace transform of the channel coefficient G and $I_3 \triangleq \mathbb{E}_G\left[(sG)^\delta\gamma(1-\delta,sG)\right]$.

For κ-μ fading, the integral I_3 can be evaluated as follows

$$\begin{aligned} I_3 &= (s\Omega)^\delta(\mu\kappa)^{\frac{1-\mu}{2}}\mathrm{e}^{-\mu\kappa} \\ &\quad\times\int_0^\infty t^{\delta+\frac{\mu-1}{2}}\gamma(1-\delta,s\Omega t)\mathrm{I}_{\mu-1}\left(2\sqrt{\mu\kappa t}\right)\mathrm{e}^{-t}\mathrm{d}t \\ &= \frac{s\Omega\cdot\mathrm{e}^{-\mu\kappa}}{(1-\delta)\Gamma(\mu)} \\ &\quad\times\int_0^\infty t^\mu\mathrm{e}^{-(1+s\Omega)t}{}_1F_1(1;2-\delta;s\Omega t){}_0F_1(;\mu;\mu\kappa t)\mathrm{d}t \\ &= \frac{s\Omega\mu\cdot\mathrm{e}^{-\mu\kappa}}{(1-\delta)}{}_2F_1(\mu+1,1-\delta;2-\delta;-s\Omega), \end{aligned} \tag{53}$$

where we applied (9) with $\Omega_{\kappa\mu} = \frac{\bar{w}}{\mu(1+\kappa)}$ in the first equality, utilized (35) in the second equality, then used (37), (39) and (40) in the last equality. By substituting $\mathcal{L}_G(s)$ of (9), (51), (52), (53) to (48), we obtain (16) for the κ-μ distribution.

Similarly for η-μ fading,

$$\begin{aligned} I_3 &= \frac{s^\delta}{h^\mu}\sum_{n=0}^\infty\left(\frac{H}{h}\right)^{2n}\binom{n+\mu-1}{\mu-1}\frac{\Omega^{-2n-2\mu}}{\Gamma(2n+2\mu)} \\ &\quad\times\int_0^\infty x^{\delta+2n+2\mu-1}\gamma(1-\delta,sx)\mathrm{e}^{-\frac{x}{\Omega}}\mathrm{d}x \\ &= \frac{s\Omega}{h^\mu(1-\delta)}\sum_{n=0}^\infty(2n+2\mu)\left(\frac{H}{h}\right)^{2n}\binom{n+\mu-1}{\mu-1} \\ &\quad\times{}_2F_1(1,1-\delta-2n-2\mu;2-\delta;-s\Omega) \\ &= \frac{2s\Omega h^\mu}{(1-\delta)H^{2\mu}}\sum_{n'=\mu}^\infty n'\left(\frac{H}{h}\right)^{2n'}\binom{n'-1}{\mu-1} \\ &\quad\times{}_2F_1(1,1-\delta-2n';2-\delta;-s\Omega), \end{aligned} \tag{54}$$

where we used the series representation of the Bessel function (36) in the first equality, applied (34) in the second equality and used a change of variable, *i.e.*, $n+\mu = n'$, in the last equality. The corresponding Laplace transform of interference over η-μ fading can be obtained by substituting $\mathcal{L}_G(s)$ of (10), (51), (52), (54) to (48). This completes the proof.

Appendix V

In this appendix, we provide a proof for Theorem 1. First, we consider κ-μ fading and obtain the series representation of the κ-μ distribution by using (9) and (36) as follows

$$f_G(x) = \frac{1}{\mathrm{e}^{\mu\kappa}}\sum_{n=0}^\infty\frac{(\mu\kappa)^n}{n!}\frac{\Omega^{-n-\mu}}{\Gamma(n+\mu)}x^{n+\mu-1}\exp\left(-\frac{x}{\Omega}\right). \tag{55}$$

Then, the average of an arbitrary function of the SINR $\gamma = \frac{G_0}{I+N}$ for a given interference I is

$$\begin{aligned} \mathbb{E}\left[g\left(\frac{G_0}{I+N}\right)\middle|I\right] &= \frac{1}{\mathrm{e}^{\mu\kappa}}\sum_{n=0}^\infty\frac{(\mu\kappa)^n}{n!} \\ &\quad\times\int_0^\infty\frac{x^{\mu+n-1}}{\Gamma(\mu+n)}g\left(\frac{x}{I+N}\right)\Omega^{-n-\mu}\exp\left(-\frac{x}{\Omega}\right)\mathrm{d}x \\ &= \frac{1}{\mathrm{e}^{\mu\kappa}}\sum_{n=0}^\infty\frac{(\mu\kappa)^n}{n!}\int_0^\infty\frac{z^{\mu+n-1}}{\Gamma(\mu+n)}g(z)\,b^{\mu+n}\mathrm{e}^{-bz}\mathrm{d}z, \end{aligned} \tag{56}$$

where we applied (55) in the first equality and used a change of variable, *i.e.*, $\frac{x}{I+N} = z$ and $b = \frac{(I+N)}{\Omega}$, in the second equality. The integral in (56) can be evaluated as follows

$$\int_0^\infty \underbrace{\frac{z^{\mu+n-1}}{\Gamma(\mu+n)} g(z)}_{u} \underbrace{b^{\mu+n} \mathrm{e}^{-bz}}_{v'} \mathrm{d}z = -\sum_{i=0}^{\mu+n-1} g_i(z) b^{\mu+n-i-1} \mathrm{e}^{-bz} \Big|_0^\infty + \int_0^\infty g_{\mu+n}(z) \mathrm{e}^{-bz} \mathrm{d}z, \tag{57}$$

where we applied integration by parts $\mu + n$ times, defined $g_i(z)$ in (19), and

$$g_i(0) = \begin{cases} 0, & \text{for } i < \mu + n - 1 \\ g(0), & \text{for } i = \mu + n - 1 \end{cases}. \tag{58}$$

Then, the average of an arbitrary function of the SINR for the κ-μ fading is given by

$$\begin{aligned} \mathbb{E}\left[g\left(\frac{G_0}{I+N} \right) \right] &= \mathbb{E}\left[\mathbb{E}\left[g\left(\frac{G_0}{I+N} \right) \Big| I \right] \right] \\ &= g(0) + \frac{1}{\mathrm{e}^{\mu\kappa}} \sum_{n=0}^{\infty} \frac{(\mu\kappa)^n}{n!} \varphi_{\kappa\mu}(n), \end{aligned} \tag{59}$$

where we applied $\frac{1}{\mathrm{e}^{\mu\kappa}} \sum_{n=0}^{\infty} \frac{(\mu\kappa)^n}{n!} = 1$. Similarly, (20) can be evaluated for η-μ fading by repeatedly applying integration by parts. This completes the proof.

APPENDIX VI

In this appendix, we express the CDF of the κ-μ and η-μ distributions using a series representation. First, we integrate the PDF of the κ-μ distribution in (55) as follows

$$\begin{aligned} F_G(x) = \int_0^x f_G(t) \mathrm{d}t &= \frac{1}{\mathrm{e}^{\mu\kappa}} \sum_{n=0}^{\infty} \frac{(\mu\kappa)^n}{n!} \frac{\gamma\left(n+\mu, \frac{x}{\Omega}\right)}{\Gamma(n+\mu)} \\ &= \sum_{n=0}^{\infty} \sum_{m=0}^{\infty} \frac{(\mu\kappa)^n \mathrm{e}^{-\mu\kappa}}{n! \cdot \Gamma(n+\mu+m+1)} \left(\frac{x}{\Omega} \right)^{n+\mu+m} \mathrm{e}^{-\frac{x}{\Omega}} \\ &= \sum_{n=0}^{\infty} \sum_{m=0}^{\infty} b_{n,m}^{\kappa\mu} \left(\frac{x}{\Omega} \right)^{n+\mu+m} \exp\left(-\frac{x}{\Omega} \right), \end{aligned} \tag{60}$$

where we used the definition of the incomplete gamma function $\gamma(s,x) = \int_0^x t^{s-1} \mathrm{e}^{-t} \mathrm{d}t$ in the second equality, applied (36) in the third equality, denoted $\Omega_{\kappa\mu} = \frac{\tilde{w}}{\mu(1+\kappa)}$ and $b_{n,m}^{\kappa\mu} \triangleq \frac{(\mu\kappa)^n \mathrm{e}^{-\mu\kappa}}{n! \cdot \Gamma(n+\mu+m+1)}$. Similarly, for the η-μ distribution, the series representation of its CDF is given by

$$\begin{aligned} F_G(x) &= \frac{1}{h^\mu} \sum_{n=0}^{\infty} \left(\frac{H}{h} \right)^{2n} \binom{n+\mu-1}{\mu-1} \frac{\gamma\left(2n+2\mu, \frac{x}{\Omega}\right)}{\Gamma(2n+2\mu)} \\ &= \sum_{n=0}^{\infty} \sum_{m=0}^{\infty} b_{n,m}^{\eta\mu} \left(\frac{x}{\Omega} \right)^{m+2n+2\mu} \exp\left(-\frac{x}{\Omega} \right), \end{aligned} \tag{61}$$

where $b_{n,m}^{\eta\mu} \triangleq \frac{1}{h^\mu} \left(\frac{H}{h} \right)^{2n} \binom{n+\mu-1}{\mu-1} \frac{1}{\Gamma(2n+2\mu+m+1)}$.

REFERENCES

[1] "5G use cases and requirements," Nokia Netw., White Paper, 2014.

[2] M. N. Tehrani, M. Uysal, and H. Yanikomeroglu, "Device-to-device communication in 5G cellular networks: Challenges, solutions, and future directions," *IEEE Commun. Mag.*, vol. 52, no. 5, pp. 86–92, May 2014.

[3] A. Asadi, Q. Wang, and V. Mancuso, "A survey on device-to-device communication in cellular networks," *IEEE Commun. Surveys Tuts.*, vol. 16, no. 4, pp. 1801–1819, 4th Quart., 2014.

[4] 3GPP, "3rd generation partnership project; technical specification group services and system aspects; Feasibility study for proximity services (ProSe) (Release 12)," 3GPP, Tech. Rep. TR 22.803 V12.2.0, Jun. 2013.

[5] Y.-D. Lin and Y.-C. Hsu, "Multihop cellular: A new architecture for wireless communications," in *Proc. 19th Annu. Joint Conf. IEEE Comput. Commun. Soc. (INFOCOM)*, vol. 3. Mar. 2000, pp. 1273–1282.

[6] B. Kaufman and B. Aazhang, "Cellular networks with an overlaid device to device network," in *Proc. 42nd Asilomar Conf. IEEE Signals, Syst. Comput.*, Oct. 2008, pp. 1537–1541.

[7] K. Doppler, M. Rinne, C. Wijting, C. B. Ribeiro, and K. Hugl, "Device-to-device communication as an underlay to LTE-advanced networks," *IEEE Commun. Mag.*, vol. 47, no. 12, pp. 42–49, Dec. 2009.

[8] B. Zhou, H. Hu, S. Q. Huang, and H. H. Chen, "Intracluster device-to-device relay algorithm with optimal resource utilization," *IEEE Trans. Veh. Technol.*, vol. 62, no. 5, pp. 2315–2326, Jun. 2013.

[9] S.-Y. Lien, K.-C. Chen, and Y. Lin, "Toward ubiquitous massive accesses in 3GPP machine-to-machine communications," *IEEE Commun. Mag.*, vol. 49, no. 4, pp. 66–74, Apr. 2011.

[10] X. Bao, U. Lee, I. Rimac, and R. R. Choudhury, "DataSpotting: Offloading cellular traffic via managed device-to-device data transfer at data spots," *ACM SIGMOBILE Mobile Comput. Commun. Rev.*, vol. 14, no. 3, p. 37, Dec. 2010.

[11] H. A. Mustafa, M. Z. Shakir, Y. A. Sambo, K. A. Qaraqe, M. A. Imran, and E. Serpedin, "Spectral efficiency improvements in HetNets by exploiting device-to-device communications," in *Proc. IEEE Globecom Workshops (GC Wkshps)*, Dec. 2014, pp. 857–862.

[12] M. Haenggi, *Stochastic Geometry for Wireless Networks*, vol. 1. Cambridge, U.K.: Cambridge Univ. Press, 2012.

[13] J. G. Andrews, A. K. Gupta, and H. S. Dhillon. (2016). "A primer on cellular network analysis using stochastic geometry." [Online]. Available: http://arxiv.org/abs/1604.03183

[14] J. G. Andrews, F. Baccelli, and R. K. Ganti, "A tractable approach to coverage and rate in cellular networks," *IEEE Trans. Commun.*, vol. 59, no. 11, pp. 3122–3134, Nov. 2011.

[15] H.-S. Jo, Y. J. Sang, P. Xia, and J. G. Andrews, "Heterogeneous cellular networks with flexible cell association: A comprehensive downlink SINR analysis," *IEEE Trans. Wireless Commun.*, vol. 11, no. 10, pp. 3484–3494, Oct. 2012.

[16] H. S. Dhillon, R. K. Ganti, F. Baccelli, and J. G. Andrews, "Modeling and analysis of K-tier downlink heterogeneous cellular networks," *IEEE J. Sel. Areas Commun.*, vol. 30, no. 3, pp. 550–560, Apr. 2012.

[17] Y. J. Chun, M. O. Hasna, and A. Ghrayeb, "Modeling heterogeneous cellular networks interference using Poisson cluster processes," *IEEE J. Sel. Areas Commun.*, vol. 33, no. 10, pp. 2182–2195, Oct. 2015.

[18] X. Lin, J. G. Andrews, and A. Ghosh, "Spectrum sharing for device-to-device communication in cellular networks," *IEEE Trans. Wireless Commun.*, vol. 13, no. 12, pp. 6727–6740, Dec. 2014.

[19] G. George, R. K. Mungara, and A. Lozano, "An analytical framework for device-to-device communication in cellular networks," *IEEE Trans. Wireless Commun.*, vol. 14, no. 11, pp. 6297–6310, Nov. 2015.

[20] H. ElSawy, E. Hossain, and M. S. Alouini, "Analytical modeling of mode selection and power control for underlay D2D communication in cellular networks," *IEEE Trans. Commun.*, vol. 62, no. 11, pp. 4147–4161, Nov. 2014.

[21] M. Peng, Y. Li, T. Q. S. Quek, and C. Wang, "Device-to-device underlaid cellular networks under Rician fading channels," *IEEE Trans. Wireless Commun.*, vol. 13, no. 8, pp. 4247–4259, Aug. 2014.

[22] J. Medbo *et al.*, "Channel modelling for the fifth generation mobile communications," in *Proc. 8th Eur. Conf. Antennas Propag. (EuCAP)*, Apr. 2014, pp. 219–223.

[23] M. Yacoub, "The $\kappa - \mu$ distribution and the $\eta - \mu$ distribution," *IEEE Antennas Propag. Mag.*, vol. 49, no. 1, pp. 68–81, Feb. 2007.

[24] D. B. Da Costa and M. D. Yacoub, "Moment generating functions of generalized fading distributions and applications," *IEEE Commun. Lett.*, vol. 12, no. 2, pp. 112–114, Feb. 2008.

[25] S. L. Cotton, "Human body shadowing in cellular device-to-device communications: Channel modeling using the shadowed κ-μ fading model," *IEEE J. Sel. Areas Commun.*, vol. 33, no. 1, pp. 111–119, Jan. 2015.
[26] D. B. da Costa and M. D. Yacoub, "The $\eta - \mu$ joint phase-envelope distribution," *IEEE Antennas Wireless Propag. Lett.*, vol. 6, pp. 195–198, 2007.
[27] B. Blaszczyszyn and H. P. Keeler, "Equivalence and comparison of heterogeneous cellular networks," in *Proc. IEEE Int. Symp. Pers. Indoor Mobile Radio Commun. (PIMRC)*, Sep. 2013, pp. 153–157.
[28] H. P. Keeler, B. Blaszczyszyn, and M. K. Karray, "SINR-based k-coverage probability in cellular networks with arbitrary shadowing," in *Proc. IEEE Int. Symp. Inf. Theory*, Jul. 2013, pp. 1167–1171.
[29] H. S. Dhillon and J. G. Andrews, "Downlink rate distribution in heterogeneous cellular networks under generalized cell selection," *IEEE Wireless Commun. Lett.*, vol. 3, no. 1, pp. 42–45, Feb. 2014.
[30] X. Zhang and M. Haenggi, "A stochastic geometry analysis of inter-cell interference coordination and intra-cell diversity," *IEEE Trans. Wireless Commun.*, vol. 13, no. 12, pp. 6655–6669, Dec. 2014.
[31] R. Tanbourgi, H. S. Dhillon, J. G. Andrews, and F. K. Jondral, "Dual-branch MRC receivers under spatial interference correlation and Nakagami fading," *IEEE Trans. Commun.*, vol. 62, no. 6, pp. 1830–1844, Jun. 2014.
[32] G. Miel and R. Mooney, "On the condition number of Lagrangian numerical differentiation," *Appl. Math. Comput.*, vol. 16, no. 3, pp. 241–252, 1985.
[33] M. Di Renzo and P. Guan, "A mathematical framework to the computation of the error probability of downlink MIMO cellular networks by using stochastic geometry," *IEEE Trans. Commun.*, vol. 62, no. 8, pp. 2860–2879, Aug. 2014.
[34] F. Baccelli, B. Błaszczyszyn, and P. Mühlethaler, "Stochastic analysis of spatial and opportunistic Aloha," *IEEE J. Sel. Areas Commun.*, vol. 27, no. 7, pp. 1105–1119, Sep. 2009.
[35] Y. Kim, F. Baccelli, and G. de Veciana, "Spatial reuse and fairness of ad hoc networks with channel-aware CSMA protocols," *IEEE Trans. Inf. Theory*, vol. 60, no. 7, pp. 4139–4157, Jul. 2014.
[36] M. Haenggi, "User point processes in cellular networks," *IEEE Wireless Commun. Lett.*, vol. 6, pp. 258–261, Apr. 2017.
[37] B. Błaszczyszyn and D. Yogeshwaran, "Clustering comparison of point processes, with applications to random geometric models," in *Stochastic Geometry, Spatial Statistics and Random Fields: Models and Algorithms* (Lecture Notes in Mathematics), vol. 2120, V. Schmidt, Ed. Springer, 2014, ch. 2, pp. 31–71.
[38] S. Singh, X. Zhang, and J. G. Andrews, "Joint rate and SINR coverage analysis for decoupled uplink-downlink biased cell associations in HetNets," *IEEE Trans. Wireless Commun.*, vol. 14, no. 10, pp. 5360–5373, Oct. 2015.
[39] D. Malak, H. S. Dhillon, and J. G. Andrews, "Optimizing data aggregation for uplink machine-to-machine communication networks," *IEEE Trans. Commun.*, vol. 64, no. 3, pp. 1274–1290, Mar. 2016.
[40] H. H. Yang, G. Geraci, and T. Q. S. Quek, "Energy-efficient design of MIMO heterogeneous networks with wireless backhaul," *IEEE Trans. Wireless Commun.*, vol. 15, no. 7, pp. 4914–4927, Jul. 2016.
[41] N. Ermolova, "Moment generating functions of the generalized η-μ and κ-μ distributions and their applications to performance evaluations of communication systems," *IEEE Commun. Lett.*, vol. 12, no. 7, pp. 502–504, Jul. 2008.
[42] K. A. Hamdi, "A useful technique for interference analysis in Nakagami fading," *IEEE Trans. Commun.*, vol. 55, no. 6, pp. 1120–1124, Jun. 2007.
[43] M. Di Renzo, A. Guidotti, and G. E. Corazza, "Average rate of downlink heterogeneous cellular networks over generalized fading channels: A stochastic geometry approach," *IEEE Trans. Commun.*, vol. 61, no. 7, pp. 3050–3071, Jul. 2013.
[44] H. Al-Hmood and H. Al-Raweshidy, "Unified modeling of composite κ-μ/gamma, η-μ/gamma, and α-μ/gamma fading channels using a mixture gamma distribution with applications to energy detection," *IEEE Antennas Wireless Propag. Lett.*, vol. 16, pp. 104–108, 2016.
[45] H. N. Huang, S. A. M. Marcantognini, and N. J. Young, "Chain rules for higher derivatives," *Math. Intell.*, vol. 28, no. 2, pp. 61–69, 2006.
[46] H. S. Dhillon, M. Kountouris, and J. G. Andrews, "Downlink MIMO HetNets: Modeling, ordering results and performance analysis," *IEEE Trans. Wireless Commun.*, vol. 12, no. 10, pp. 5208–5222, Oct. 2013.
[47] I. S. Gradshteyn and I. M. Ryzhik, *Table of Integrals, Series, and Products*, 5th ed. San Diego, CA, USA: Academic, 1994.
[48] N. Saad and R. L. Hall, "Integrals containing confluent hypergeometric functions with applications to perturbed singular potentials," *J. Phys. A, Math. General*, vol. 36, no. 28, p. 7771, Jun. 2003, doi: 10.1088/0305-4470/36/28/307.
[49] J. M. Howie, *Real Analysis* (Springer Undergraduate Mathematics Series), vol. 1. London, U.K.: Springer, 2001.

Young Jin Chun (M'12) received the B.S. degree from Yonsei University, Seoul, South Korea, in 2004, the M.S. degree from the University of Michigan, Ann Arbor, in 2007, and the Ph.D. degree from Iowa State University, Ames, in 2011, all in electrical engineering. He was a Post-Doctoral Researcher with Sungkyunkwan University, Suwon, South Korea, from 2011 to 2012, and with Qatar University, Doha, Qatar, from 2013 to 2014. In 2015, he joined Queen's University Belfast, U.K. as a Research Fellow. His research interests are primarily in the area of wireless communications with emphasis on stochastic geometry, system-level network analysis, device-to-device communications, and various use cases of 5G communications.

Simon L. Cotton (S'04–M'07–SM'14) received the B.Eng. degree in electronics and software from Ulster University, Ulster, U.K., in 2004, and the Ph.D. degree in electrical and electronic engineering from the Queen's University of Belfast, Belfast, U.K., in 2007. He is currently a Reader of Wireless Communications with the Institute of Electronics, Communications and Information Technology, Queen's University Belfast, and also a Co-Founder and the Chief Technology Officer with ActivWireless Ltd., Belfast. He has authored and co-authored over 100 publications in major IEEE/IET journals and refereed international conferences, two book chapters, and two patents. Among his research interests are cellular device-to-device, vehicular, and body-centric communications. His other research interests include radio channel characterization and modeling and the simulation of wireless channels. He was a recipient of the H. A. Wheeler Prize, in 2010, from the IEEE Antennas and Propagation Society for the best applications journal paper in the IEEE TRANSACTIONS ON ANTENNAS AND PROPAGATION in 2009. In 2011, he was a recipient of the Sir George Macfarlane Award from the U.K. Royal Academy of Engineering in recognition of his technical and scientific attainment since graduating from his first degree in engineering.

Harpreet S. Dhillon (S'11–M'13) received the B.Tech. degree in Electronics and Communication Engineering from IIT Guwahati, India, in 2008; the M.S. degree in Electrical Engineering from Virginia Tech, Blacksburg, VA, USA, in 2010; and the Ph.D. degree in Electrical Engineering from the University of Texas at Austin, TX, USA, in 2013. After a postdoctoral year at the University of Southern California (USC), Los Angeles, CA, USA, he joined Virginia Tech in August 2014, where he is currently an Assistant Professor of Electrical and Computer Engineering. He has held internships at Alcatel-Lucent Bell Labs in Crawford Hill, NJ, USA; Samsung Research America in Richardson, TX, USA; Qualcomm Inc. in San Diego, CA, USA; and Cercom, Politecnico di Torino in Italy. His research interests include communication theory, stochastic geometry, geolocation, and wireless *ad hoc* and heterogeneous cellular networks.

Dr. Dhillon has been a co-author of five best paper award recipients including the 2016 IEEE Communications Society (ComSoc) Heinrich Hertz Award, the 2015 IEEE ComSoc Young Author Best Paper Award, the 2014 IEEE ComSoc Leonard G. Abraham Prize, the 2014 European Wireless Best Student Paper Award, and the 2013 IEEE International Conference in Communications Best Paper Award in the Wireless Communications Symposium. He was also the recipient of the USC Viterbi Postdoctoral Fellowship, the 2013 UT Austin Wireless Networking and Communications Group (WNCG) leadership award, the UT Austin Microelectronics and Computer Development (MCD) Fellowship, and the 2008 Agilent Engineering and Technology Award. He is currently an Editor of the IEEE TRANSACTIONS ON WIRELESS COMMUNICATIONS, the IEEE TRANSACTIONS ON GREEN COMMUNICATIONS AND NETWORKING, and the IEEE WIRELESS COMMUNICATIONS LETTERS.

Ali Ghrayeb (SM'06) received the Ph.D. degree in electrical engineering from the University of Arizona, Tucson, USA, in 2000.

He is currently a Professor with the Department of Electrical and Computer Engineering, Texas A&M University at Qatar. He is a co-recipient of the IEEE Globecom 2010 Best Paper Award. He is the coauthor of the book *Coding for MIMO Communication Systems* (Wiley, 2008). His research interests include wireless and mobile communications, physical layer security, massive MIMO, wireless cooperative networks, and ICT for health applications.

Dr. Ghrayeb served as an instructor or co-instructor in technical tutorials at several major IEEE conferences. He served as the Executive Chair of the 2016 IEEE WCNC conference, and as the TPC co-chair of the Communications Theory Symposium at the 2011 IEEE Globecom. He serves as an Editor for the IEEE TRANSACTIONS ON COMMUNICATIONS. He has served on the editorial board of several IEEE and non-IEEE journals.

Mazen O. Hasna (SM'07) received the B.S. degree from Qatar University, Doha, Qatar, in 1994, the M.S. degree from the University of Southern California, Los Angeles, CA, USA, in 1998, and the Ph.D. degree from the University of Minnesota, Twin Cities, Minneapolis, MN, USA, in 2003, all in electrical engineering.

In 2003, he joined the Department of Electrical Engineering, Qatar University, where he is currently an Associate Professor. His research interests include the general area of digital communication theory and its application to the performance evaluation of wireless communication systems over fading channels. His current specific research interests include cooperative communications, ad hoc networks, cognitive radios, and network coding.